


Transition metal complexes of novel binuclear Schiff base derived from 3,3'-diaminobenzidine: synthesis, characterization, thermal behavior, DFT, antimicrobial and molecular docking studies

Venkittapuram Palaniswamy Radha, Subramanian Chitra, Suyambulingam Jonekirubavathi, Ill-Min Chung, Seung-Hyun Kim & Mayakrishnan Prabakaran

To cite this article: Venkittapuram Palaniswamy Radha, Subramanian Chitra, Suyambulingam Jonekirubavathi, Ill-Min Chung, Seung-Hyun Kim & Mayakrishnan Prabakaran (2020): Transition metal complexes of novel binuclear Schiff base derived from 3,3'-diaminobenzidine: synthesis, characterization, thermal behavior, DFT, antimicrobial and molecular docking studies, Journal of Coordination Chemistry, DOI: [10.1080/00958972.2020.1752372](https://doi.org/10.1080/00958972.2020.1752372)


To link to this article: <https://doi.org/10.1080/00958972.2020.1752372>

 View supplementary material [↗](#)

 Published online: 21 Apr 2020.

 Submit your article to this journal [↗](#)


 Article views: 3

 View related articles [↗](#)

 View Crossmark data [↗](#)



Transition metal complexes of novel binuclear Schiff base derived from 3,3'-diaminobenzidine: synthesis, characterization, thermal behavior, DFT, antimicrobial and molecular docking studies

Venkittapuram Palaniswamy Radha^a, Subramanian Chitra^b, Suyambulingam Jonekirubavathi^b, Ill-Min Chung^c, Seung-Hyun Kim^c and Mayakrishnan Prabakaran^c 

^aDepartment of Chemistry, Jansons Institute of Technology, Coimbatore, Tamil Nadu, India;

^bDepartment of Chemistry, P.S.G.R. Krishnammal College for Women, Coimbatore, Tamil Nadu, India;

^cDepartment of Crop Science, College of Sanghur Life Science, Konkuk University, Seoul, South Korea

ABSTRACT

A series of binuclear Co(II), Ni(II), Cu(II), and Zn(II) complexes were prepared with a novel bidentate Schiff base ligand derived by condensation of 3,3'-diaminobenzidine with creatinine. The prepared compounds were characterized by elemental analysis, magnetic susceptibility measurements, molar conductivity, FT-IR, UV-vis, ¹H NMR, ¹³C NMR and mass spectra and thermal analysis (TGA/DTG). From spectral analysis, an octahedral geometry was proposed for the complexes except Zn(II) complex which had tetrahedral geometry. The microcrystalline nature of the complexes has been confirmed by powder XRD and SEM analyses. The molecular structures of the Schiff base L and its Zn(II) complex were fully optimized and also their quantum chemical parameters were calculated. The synthesized ligand and their metal complexes were screened against two gram-positive, gram-negative bacterial and fungal species. The results revealed that the metal complexes exhibited higher antimicrobial activity than the free ligand. The antioxidant activity of the synthesized ligand and their metal complexes was carried out by DPPH method.

ARTICLE HISTORY


Received 22 March 2019
Accepted 24 March 2020

KEYWORDS

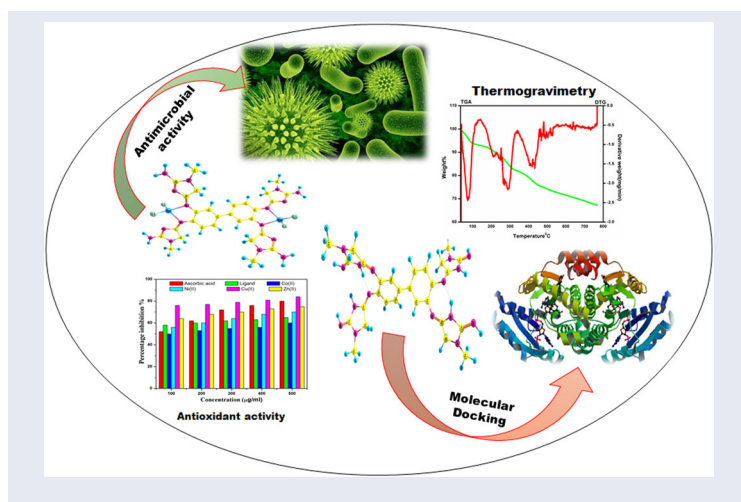
Binuclear; Schiff base ligand; DFT studies; antimicrobial; antioxidant

CONTACT Mayakrishnan Prabakaran  prabakaranmitt@gmail.com  Department of Crop Science, College of Sanghur Life Science, Konkuk University, Seoul 05029, South Korea

*Venkittapuram Palaniswamy Radha and Ill-Min Chung contributed equally to this work.

 Supplemental data for this article can be accessed [here](#).

© 2020 Informa UK Limited, trading as Taylor & Francis Group



1. Introduction

The synthesized pharmaceutical compounds in the past decade contain five-, six-, and seven-membered rings such as piperidines, imidazoles, piperazines and many other heterocycles containing sulfur, nitrogen or oxygen atoms. These heterocyclic compounds exhibit a wide range of physiological properties including analgesic, anti-hypertensive, and anti-cancer activities. Sulfur, nitrogen, oxygen, amino-nitrogen, azomethine nitrogen, alcoholic, and phenolic oxygen are the main donor atoms of the heterocyclic systems. These compounds are used to model significant bio-inorganic systems. Schiff base ligands containing these heterocyclic rings have earned much attention in coordination chemistry in recent years.

Metal ions play a major role in biological processes. The incorporation of metal ions into the biological systems in treatment of diseases is the main subdivision in the field of bioinorganic chemistry [1]. A metal ion can easily lose electron and become positively charged, which makes it soluble in biological fluids. They play their role in biological systems as positively charged ions. The biological molecules such as protein and DNA are electron rich, which can easily bind to the electron deficient metal ions and interact with them easily [2, 3].

The biological properties of the ligands and the metal moiety have been drastically modified by chelation [4]. The binucleating imino ligands are versatile and they reveal very rich coordination chemistry. A substantial effort is currently being investigated in the development of such chelating ligands. Such species occupy an important position in modern inorganic chemistry [5–7] and the complexation ability towards transition metals. Schiff base ligands play a vital role in transition metal coordination chemistry [8, 9]. Binuclear Schiff base transition metal complexes play a major role as biological models, catalysts for organic reactions and components in the formation of new materials [10].

The azomethine linkage of Schiff bases is responsible for the biological activities such as treatment of cancer [11], as antibacterial [12], antiviral agent [13, 14], and

other biological properties [15]. These complexes have several applications in absorption, chemical analysis, heterogeneous, and homogeneous catalysis, in pesticides, for oxidation and polymerization of organic compounds [16–18]. In recent years, nonplatinum-based metal therapeutics, in particular late 3d transition metal ions *viz.* Co(II), Ni(II), Cu(II), and Zn(II), are endogenously compatible to the living systems [19]. Those Schiff bases which form binuclear transition metal complexes are useful in studying the relation between structures and magnetic exchange interaction and to mimic bimetallic biosites in various proteins and enzymes [20, 21]. Copper is a biologically relevant element and many enzymes that depend on copper for their activity have been identified. Zinc is essential to all forms of life and a large number of diseases and congenital disorders have been traced to zinc deficiency. Zinc is a natural component of insulin and it controls sugar metabolism. In this regard, there is a great interest in binucleating Schiff base ligands and their transition metal complexes.

Based on the above facts, we have designed a new binucleating Schiff base ligand incorporating inidazoline moiety. The present work deals with the synthesis of a novel Schiff base ligand by condensation of 3,3'-diaminobenzidine and creatinine and its binuclear Co(II), Ni(II), Cu(II), and Zn(II) complexes. The prepared ligand and its complexes were characterized using different physicochemical techniques. The thermal decomposition of the metal complexes was analyzed. The microcrystalline nature of the complexes was determined by powder XRD. DFT calculations were performed at B3LYP/LANL2DZ level for ligand and complex **4**. The antimicrobial activities of the synthesized ligand and its metal complexes were screened against gram-positive, gram-negative bacterial, and fungal species. The antioxidant activity of the ligand and the metal complexes was studied by DPPH assay method.

2. Experimental methods

2.1. Materials and reagents

All the chemicals used were AR grade and of high purity. Creatinine (Sigma Aldrich), 3,3'-diaminobenzidine (Sigma Aldrich) and metal salts (Sigma Aldrich) were used as received. All the organic solvents were purchased from Merck and used without purification.

2.2. Physical measurements

The FT-IR spectra were recorded on a Shimadzu IR affinity 1 spectrophotometer from 4000 to 400 cm^{-1} . The magnetic susceptibility of the complexes was measured on powdered samples using Gouy's method. Molar conductivities of 10^{-3} M solutions of the complexes in DMSO were measured using an Elico digital conductivity meter (model CM180) having a dip type cell calibrated with KCl solution. Microanalysis of carbon, hydrogen and nitrogen were carried out on an Elementer Vario EL III CHN analyzer at STIC Cochin. Estimation of metals was carried out by standard EDTA solution. ^1H NMR spectra was recorded in DMSO- d_6 using a Bruker Avance III 400 MHz FT – digital NMR spectrometer. The mass spectra were recorded using a Shimadzu LC20AD mass spectrometer. The thermal analysis (TG/DTG) of the solid complexes was carried

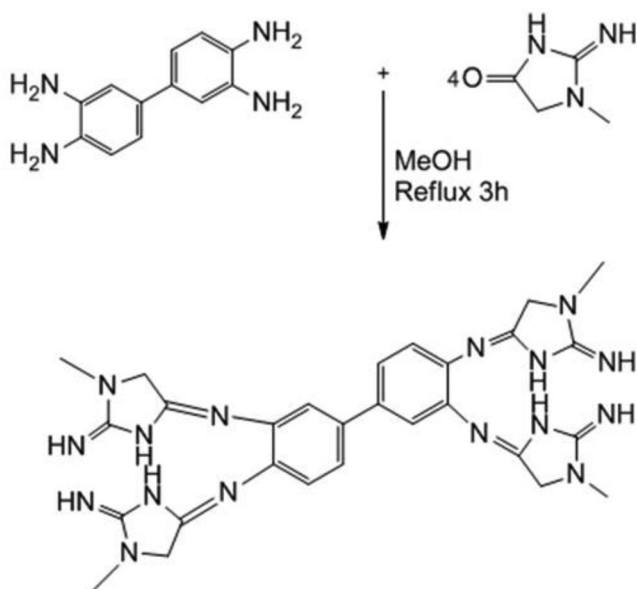


Figure 1. Synthesis of Schiff base ligand (L).

out from room temperature to 800 °C using a Perkin Elmer STA 6000 thermal analyser. X-ray diffraction (XRD) patterns were recorded using a Bruker AXS D8 Advance powder X-ray diffractometer with an X-ray source: Cu and wavelength 1.5406 Å. Scanning electron microscopy with energy dispersive spectrometry (SEM/EDS) was used for morphological evaluation.

2.3. Synthesis of Schiff base ligand and their metal complexes

2.3.1. Procedure for synthesis of Schiff base ligand

The Schiff base ligand (L) was prepared by mixing 20 mL of methanolic solution of 3,3'-diaminobenzidine (1 mmol) with 10 mL of methanolic solution of creatinine (4 mmol). The mixture was heated under reflux for 3 h at 80 °C. The resulting dark brown product obtained was filtered and dried in desiccators using silica gel. The synthesis of the ligand is given in Figure 1. The brown Schiff base product was produced in 85% yield. M.P: 236 °C. Anal. Calcd for $C_{28}H_{34}N_{16}$ (%): C, 56.53; H, 5.76; N, 37.69. Found (%): C, 56.57; H, 5.74; N, 37.72. FT-IR (KBr, ν , cm^{-1}): (C=N)_{azomethine}, 1670; (C=NH), 1520; (ring NH): 3220; 1H NMR (300 MHz, DMSO- d_6), δ (ppm): 7.5-8 (m, 8H, aromatic), 3.3 (s, 12H, CH₃), 2.51 (s, 6H, methylene), 9.8 (s, 4H, NH); UV-vis (λ_{max} , nm): 238 (π - π^*), 323 (n - π^*).

2.3.2. Procedure for synthesis of metal complexes (1-4)

The Co(II), Ni(II), Cu(II), and Zn(II) complexes were prepared by the reaction of 1:2 molar mixture of ligand and metal chlorides in acetonitrile. The mixture was refluxed for about 2 h at 90 °C. The resulting product was filtered and dried in a desiccator using silica gel. The synthesis of the metal complexes is given in Figure 2.

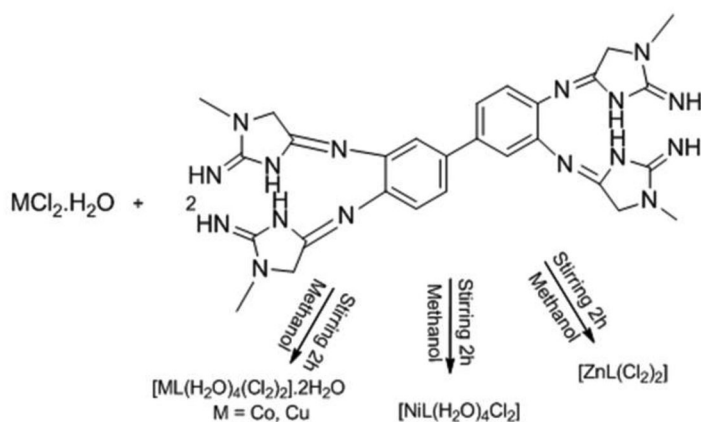


Figure 2. Synthesis of transition metal complexes.

2.3.2.1. $[Co_2L(H_2O)_4Cl_4] \cdot 2H_2O$ (1). Yield 74%; brown solid, m.p > 250 °C. Anal. Calcd for $[Co_2L(H_2O)_4Cl_4] \cdot 2H_2O$ (%): C, 34.94; H, 4.82; N, 23.28; Co, 12.25. Found (%): C, 34.94; H, 4.79; N, 23.31; Co, 12.28. IR (ν , cm^{-1}): (C=N)_{azomethine}, 1652; (NH₂), 3647, 3580; (M-N), 422; (M-Cl), 339; (H₂O coordinated), 832–841; μ_{eff} (BM): 3.76. Λ_m ($\Omega^{-1} cm^2 mol^{-1}$): 11.23.

2.3.2.2. $[Ni_2L(H_2O)_4Cl_4]$ (2). Yield 72%; dark green, m.p > 250 °C. Anal. Calcd for $[Ni_2L(H_2O)_4Cl_4]$ (%): C, 36.32; H, 4.57; N, 24.20; Ni, 12.68. Found (%): C, 36.27; H, 4.60; N, 24.17; Ni, 12.72. IR (ν , cm^{-1}): (C=N)_{azomethine}, 1645; (NH₂), 3652, 3575; (M-N), 436; (M-Cl), 343; (H₂O coordinated), 832–841; μ_{eff} (BM): 3.1. Λ_m ($\Omega^{-1} cm^2 mol^{-1}$): 12.28.

2.3.2.3. $[Cu_2L(H_2O)_4Cl_4] \cdot H_2O$ (3). Yield 76%; dark green, m.p > 250 °C. Anal. Calcd. for $[Cu_2L(H_2O)_4Cl_4] \cdot H_2O$ (%): C, 34.61; H, 4.77; N, 23.06; Cu, 13.08. Found (%): C, 34.65; H, 4.79; N, 23.02; Cu, 13.05. IR (ν , cm^{-1}): (C=N)_{azomethine}, 1638; (NH₂), 3659, 3598; (M-N), 465; (M-Cl), 363; (H₂O coordinated), 832–841; μ_{eff} (BM): 1.87. Λ_m ($\Omega^{-1} cm^2 mol^{-1}$): 14.51.

2.3.2.4. $[Zn_2LCl_4]$ (4). Yield 70%; brown, m.p > 250 °C. Anal. Calcd. for $[Zn_2LCl_4]$ (%): C, 38.78; H, 43.95; N, 25.84; Zn, 15.08. Found (%): C, 38.82; H, 3.92; N, 25.8; Zn, 15.13. IR (ν , cm^{-1}): (C=N)_{azomethine}, 1653; (NH₂), 3635, 3519; (M-N), 401; (M-Cl), 324; (H₂O coordinated), 832–841; Λ_m ($\Omega^{-1} cm^2 mol^{-1}$): 13.56.

2.4. DFT calculation

DFT calculations were performed with the Gaussian 09W program using B3LYP model [22]. The molecular geometry of L and **4** was fully optimized using density function theory based on 6–31g (d,p) basis sets except for **4** where LANL2DZ basis set was used. Chemcraft was used for visualization of the optimized structure [23]. The quantum chemical parameters such as E_{HOMO} , E_{LUMO} and energy gap (ΔE) were also calculated.

2.5. Antimicrobial activity

The antimicrobial activity of L and **1–4** was studied using paper disc diffusion method and minimum inhibitory concentration (MIC). The prepared compounds were screened against two Gram-positive bacteria, *Staphylococcus aureus* (*S. aureus*) and *Bacillus subtilis* (*B. subtilis*), two Gram-negative bacteria, *Pseudomonas aeruginosa* (*P. aeruginosa*) and *Escherichia coli* (*E. coli*), and two fungal species, *Aspergillus niger* (*A. niger*) and *Candida albicans* (*C. albicans*). Ciprofloxacin and Clotrimazole were used as standard drugs for bacteria and fungi, respectively. The microorganisms studied were grown overnight and then suspended in Muller Hinton broth to match the 0.5 McFarland standards [24]. The sterile glass spreader was used for even distribution of the inoculums. The sterile discs measuring about 6 mm soaked in known concentration of the test compounds were placed in the nutrient agar medium. The reference drug was used as positive control and solvent DMSO was used as negative control. The antimicrobial activity was assayed by measuring the diameter zone of inhibition. The minimum inhibitory concentration (MIC) values were examined by the broth microdilution method using concentrations of 1000, 250, 125, 62.5, 31.25, and 15.625 $\mu\text{g mL}^{-1}$. The cultures of the bacterial strains were incubated for 24 h at 37 °C and 48 h at 25 °C for fungi, and the growth was observed visually as well as spectrophotometrically [25].

2.6. Antioxidant activity

The synthesized compounds were examined for their antioxidant activity by 1,1-diphenylpicrylhydrazyl (DPPH) method [26]. The DPPH radical is a stable free radical having a λ_{max} at 517 nm. A stock solution of drug was diluted to final concentrations of 100, 200, 300, 400, and 500 $\mu\text{g mL}^{-1}$ in methanol. Methanolic DPPH solution (1 mL, 0.3 mmol) was then added to 3.0 mL of drug solution of various concentrations. The tube was then placed at an ambient temperature for 30 min and the absorbance was measured at 517 nm. The scavenging potential of the compounds was calculated by the formula,

$$\% \text{inhibition} = \left[\frac{A_{\text{control}} - A_{\text{sample}}}{A_{\text{control}}} \right] \times 100$$

where A_{control} is the absorbance of L-ascorbic acid (standard) and A_{sample} is the absorbance of different compounds. The methanolic DPPH solution (1 mL, 0.3 mM) was used as control. The IC_{50} can be calculated using the percentage of activity.

3. Results and discussion

3.1. Synthesis

The present work deals with the synthesis of a new Schiff base ligand. Four new Co(II), Ni(II), Cu(II), and Zn(II) binuclear complexes were synthesized from the Schiff base ligand. All the synthesized compounds were characterized by elemental analysis, FT-IR and UV-Vis spectroscopy.

3.2. FT-IR spectra

The information about the binding sites of the ligand can be obtained from the comparative study of the FT-IR spectra of ligand and their metal complexes. The IR spectra of the synthesized Schiff base ligand L showed the presence of $\nu(>C=N)$ stretching band at 1670 cm^{-1} . In the IR spectra of the complexes, the $\nu(>C=N)$ band appeared around $1638\text{--}1653\text{ cm}^{-1}$. The band shifted to lower wavenumber after complexation. This shift indicated coordination of the ligand through their imine nitrogen atoms [27]. The coordination of azomethine nitrogen to metal ion reduces the electron density of $(>C=N)$ by back-bonding from the metal to the π^* orbital of azomethine group. Further, the appearance of new bands at $400\text{--}465\text{ cm}^{-1}$ corresponding to (M-N) stretching in all the complexes also confirms coordination of the metal atoms through azomethine nitrogen atom [28, 29]. The presence of medium-intensity band at 1520 cm^{-1} of the ligand may be assigned to $\nu(C=NH)$ stretching. A band around 3220 cm^{-1} of the ligand corresponds to ring $\nu(NH)$ vibration. The disappearance of these two bands in the IR spectra of the complexes and formation of band corresponding to $\nu(NH_2)$ around $3635\text{--}3659\text{ cm}^{-1}$ and $3519\text{--}3598\text{ cm}^{-1}$ confirms the amino-imino tautomerism of the creatinine moiety, which further confirms the non-coordination of the nitrogen to the metal atoms. A band of medium intensity around $832\text{--}841\text{ cm}^{-1}$ in **1–3** suggests the presence of coordinated water [30]. A band observed around $324\text{--}363\text{ cm}^{-1}$ in the spectra of **1–4** were assigned to the M-Cl stretching [31]. The above results revealed that the Schiff base was coordinated to the metal ions in a neutral bidentate manner with NN (azomethine) nitrogen.

3.3. ^1H NMR spectra

The ^1H NMR spectra of Schiff base ligand L displayed a singlet at 9.8 ppm corresponding to NH proton. The multiplets in the region 7.5–8 ppm may be assigned to protons of aromatic rings of the ligand [32, 33]. The signals around 3.3 and 2.51 ppm in both ligand and **4** correspond to CH_3 and CH_2 protons, respectively. The disappearance of a signal at 9.8 ppm in the ^1H NMR spectra of **4** and appearance of a new signal at 8.5 ppm corresponds to NH_2 proton, indicating tautomerism of creatinine to keto-amino form.

3.4. ^{13}C NMR spectra

The ^{13}C NMR spectra of Schiff base ligand exhibited a sharp signal at 170 ppm corresponding to imine carbons [34]. The sharp signals at 39.6, 46.2, and 55.8 ppm are due to N-CH_3 and CH_2 carbons, respectively. The signals around 140 and 152 ppm may be assigned to C-N and C=NH carbons. The signals associated aromatic carbons appeared around 120–130 ppm.

3.5. Mass spectra

The formation of Schiff base ligand and its Zn(II) complex were studied with ESI-MS spectra. The molecular ion peak was observed at m/z 594.38 for the Schiff base ligand

and m/z 867.52 for the Zn(II) complex. These data are in good agreement with their molecular formula. The mass spectrum of Schiff base ligand **L** and its Zn(II) complex **4** are shown in [Supplementary material](#) Figure S1.

3.6. Molar conductance measurements

The molar conductivity (Λ_m) of 10^{-3} M solutions of all the complexes at 25 °C was determined in DMF. The results revealed that all the complexes were non-electrolytes in nature having molar conductance in the range 11.23–14.51 $\Omega^{-1} \text{ mol}^{-1} \text{ cm}^2$. This indicated that the anions were found in the coordination sphere [35, 36].

3.7. Magnetic susceptibility and electronic spectra

The ligand shows two absorption bands at 238 and 323 nm corresponding to $\pi \rightarrow \pi^*$ and $n \rightarrow \pi^*$ transitions, respectively. The $\pi \rightarrow \pi^*$ transition involves the promotion of the lone pair electron of azomethine nitrogen atom to the antibonding π -orbital associated with the azomethine group. In the metal complexes bands due to $\pi \rightarrow \pi^*$ and $n \rightarrow \pi^*$ transitions observed in the ligand was shifted to 238–245 nm and 323–332 nm, respectively. These change in the absorption shifts may be due to coordination, resulting in increased conjugation and delocalization of the whole electronic system causing an energy change in the $\pi \rightarrow \pi^*$ and $n \rightarrow \pi^*$ transitions.

The electronic spectra of **1** showed bands at 488 and 620 nm which may be assigned to ${}^4T_{1g}(F) \rightarrow {}^4T_{1g}(P)$ and ${}^4T_{1g}(F) \rightarrow {}^4A_{2g}(F)$ transitions, respectively [37]. The magnetic moment value of **1** is 3.76 BM and an octahedral geometry has been suggested for **1**.

The absorption spectrum of **2** exhibited bands at 475, 689, and 783 nm which may be assigned to ${}^3A_{2g}(F) \rightarrow {}^3T_{1g}(P)$, ${}^3A_{2g}(F) \rightarrow {}^3T_{1g}(F)$, and ${}^3A_{2g}(F) \rightarrow {}^3T_{2g}(F)$ transitions, respectively. The magnetic moment value of **2** was found to be 3.1 BM. All these data suggest an octahedral geometry for **2** [38].

The electronic spectra of **3** showed two bands at 465 and 709 nm assignable to ${}^2B_{1g} \rightarrow {}^2E_g$ and ${}^2B_{2g} \rightarrow {}^2B_{1g}$ transitions, respectively. The value of the magnetic moment of the complex was found 1.87 BM, suggesting octahedral geometry for **3** [39, 33].

Complex **4** is diamagnetic in nature, and no d-d transitions were observed for this complex. A broad band observed at 250 nm corresponds to L \rightarrow M charge transfer transition. The spectral and elemental analysis data suggest a tetrahedral geometry for **4** [40].

3.8. Powder XRD and SEM analysis

Powder X-ray diffractograms of Cu(II) and Zn(II) complexes were scanned in the range 10° – 100° at wavelength of 1.5406 Å. The diffractogram of **3** and **4** are shown in [Supplementary material](#) Figure S2. The complexes exhibit sharp peaks which indicate their crystalline nature. Using Scherrer's equation ($D = 0.9 \lambda / \beta \cos \theta$) the average crystallite size for **3** and **4** were 64 and 36 nm, respectively.

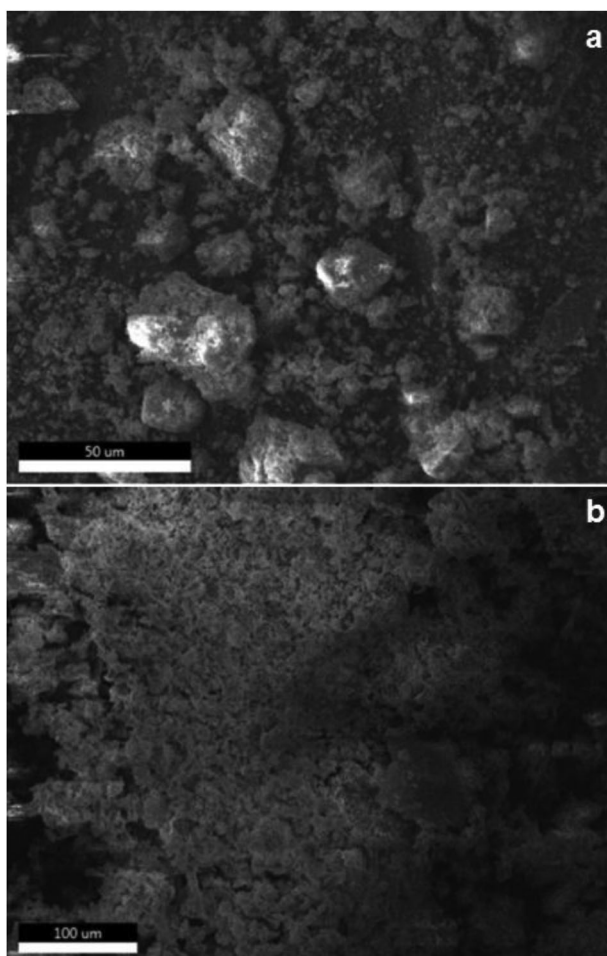


Figure 3. (a) SEM micrograph of Cu(II) complex. (b) SEM micrograph of Zn(II) complex.

The SEM pictographs of **3** and **4** shown in [Figure 3](#) exhibit a homogeneous matrix with an ideal shape of uniform phase material. Particle size of 50 μm with small cube-like shape is observed in **3**. Particle size of 100 μm with thin diamond shaped layer is observed in **4**. Based on the above analytical and spectral studies, it is confirmed that **3** and **4** have octahedral and tetrahedral geometry, respectively.

3.9. Thermo gravimetric analysis (TG and DTG)

The thermal decomposition of all the metal complexes takes place in several steps as reported in [Table 1](#) and shown in [Supplementary Material](#) Figure S3. The stability of the complexes decreases due to the presence of different groups in the organic ligand. The thermal stability of the complexes was affected by the electronegativity and atomic radius of the central metal atom. The thermogravimetric analysis was carried out from room temperature to 800 °C. The decomposition of the complexes was not completed after 800 °C.

Table 1. Thermoanalytical results (TG and DTG) of Schiff base ligand (L) and its metal complexes.

Complexes	Temp. range (°C) TG	Decomposition temp. (°C) DTG	Found mass loss Estim. (Calcd) %	Assignment
[Co ₂ L(H ₂ O) ₄ Cl ₄].2H ₂ O	45–89	68.84	4.29 (3.74)	Loss of lattice H ₂ O
	89–198	102.56	6.22 (7.49)	Loss of coordinated H ₂ O
	198–319	267.80	12.75 (14.73)	Loss due to Cl ₂
	319–766	565.39	21.37 (20.18)	Loss due to C ₈ H ₁₄ N ₆ Decomposition in progress
[Ni ₂ L(H ₂ O) ₄ Cl ₄]	84–154	145.25	9.50 (7.78)	Loss of coordinated H ₂ O
	154–362	313.89	15.35 (15.32)	Loss due to Cl ₂ Decomposition in progress
[Cu ₂ L(H ₂ O) ₄ Cl ₄].H ₂ O	55–84	79.34	3.15 (3.71)	Loss of lattice H ₂ O
	84–250	210	6.68 (7.42)	Loss of coordinated H ₂ O
	250–487	286.72, 413.17	13.53 (14.59)	Loss due to Cl ₂ Decomposition in progress
[Zn ₂ LCl ₄]	165–439	342.84	15.27 (16.35)	Loss due to Cl ₂ Decomposition in progress

The TG curve of [Co₂L(H₂O)₄Cl₄].2H₂O shows decomposition in four steps within the temperature range 45–766 °C. The first decomposition step from 45 to 89 °C with a maximum temperature at 68.84 °C with an estimated mass loss of 4.29% (calcd 3.74%) was accounted for the loss of lattice water molecules. The second decomposition step occurs from 89 to 198 °C with an estimated mass loss of 6.22% (calcd 7.49%) with maxima at 102.56 °C, which is attributed to the loss of coordinated water molecules [41]. Third decomposition from 198 to 319 °C with maximum temperature at 267.80 °C with mass loss of 12.75% (calcd 14.73%) was attributed to loss of chlorine molecules. The fourth decomposition step from 319 to 766 °C with mass loss of 21.37% (calcd 20.18%) with maxima at 565.39 °C corresponds to the loss of two creatinine moieties of the ligand molecule. The decomposition step did not finish completely. Therefore last decomposition residue was not determined [42].

The thermogram of [Ni₂L(H₂O)₄Cl₄] shows two decomposition steps from 84 to 362 °C. The first decomposition from 84 to 154 °C with maximum temperature at 145.25 °C with an estimated mass loss 9.5% (calcd 7.78%) was attributed to coordinated water molecules. The second decomposition from 154 to 362 °C with maximum temperature at 313.89 °C with an estimated mass loss 15.35% (calcd 15.32%) corresponds to the loss of chlorine molecules. The decomposition step did not finish completely. Therefore the last decomposition residue was not determined.

The TG curve of [Cu₂L(H₂O)₄Cl₄].H₂O undergoes decomposition in four steps. The first decomposition from 55 to 84 °C with maximum temperature at 79.34 °C was attributed to the loss of lattice water molecules with an estimated mass loss of 3.15% (calcd 3.71%). The second decomposition from 84 to 250 °C with an estimated mass loss of 6.68% (calcd 7.42%) with maxima at 210 °C corresponds to the loss of coordinated water molecules. The third and fourth decomposition from 250 to 487 °C with two maxima at 286.72 and 413.17 °C with mass loss of 13.53% (calcd 14.59%) was

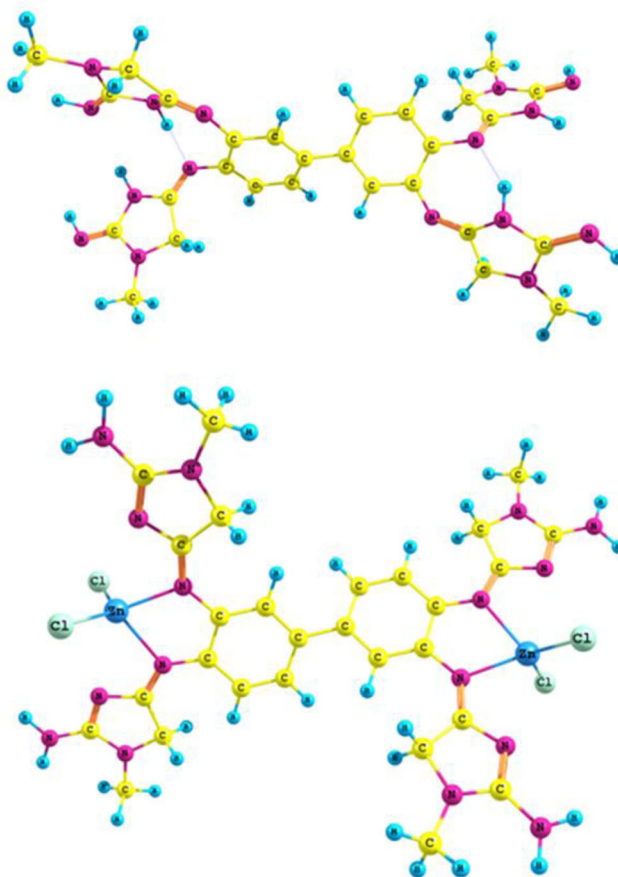


Figure 4. Optimized geometry of Schiff base ligand and Zn(II) complex.

attributed to the loss of chlorine atoms. The decomposition was incomplete hence, the final decomposition product cannot be determined.

The thermogram of $[Zn_2LCl_4]$ shows no decomposition up to 300°C , indicating the absence of lattice and coordinated water molecules [43]. The decomposition from 165 to 439°C with maximum temperature at 342.84°C with an estimated mass loss of 15.27% (calcd 16.35%) was attributed to the loss of chlorine atoms. The decomposition was incomplete. Therefore the last decomposition residue was not determined. Based on the above discussion the proposed structures of the complexes are shown in Supplementary Material Figure S4.

3.10. Geometry optimization

The molecular geometry of L and **4** were optimized in gas phase and are shown in Figure 4. The numbering scheme used to calculate bond lengths and angles for L and **4** is shown in Supplementary Material Figure S5. The values of selected bond lengths, bond angles, and torsion angles of L and Zn(II) complex are listed in Supplementary Material Table S1. A slight elongation in bond lengths C(22)-N(10), C(21)-N(9), C(14)-

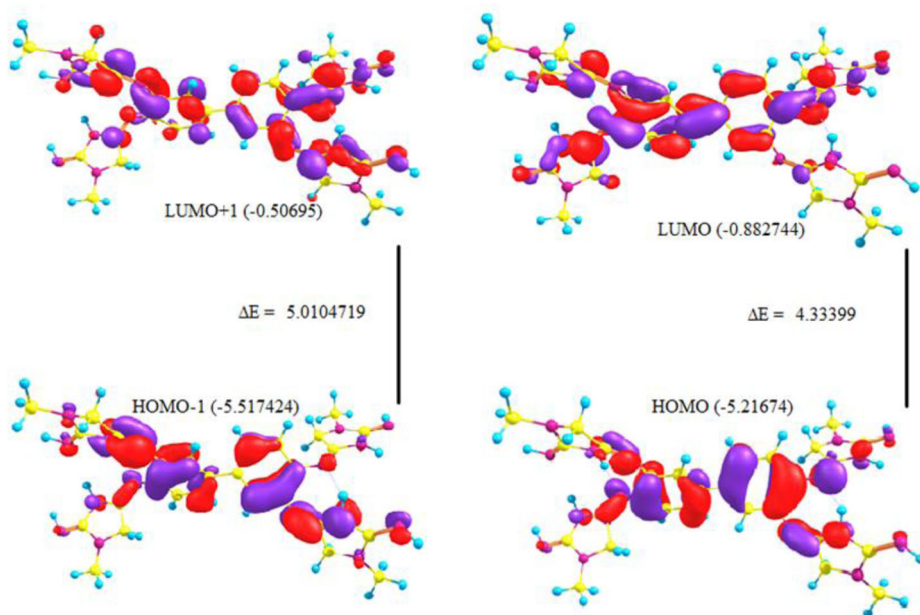


Figure 5. Frontier molecular orbital energies of Schiff base ligand.

N(2), and C(13)-N(1) was noted in Zn(II) complex as L was coordinated *via* azomethine nitrogen. The Zn(1)-N(10), Zn(1)-N(9), Zn(1)-Cl(3), Zn(1)-Cl(4), Zn(2)-N(1), Zn(2)-N(2), Zn(2)-Cl(1), and Zn(2)-Cl(2) bond lengths were 2.16, 2.16, 2.33, 2.34, 2.16, 2.16, 2.33, and 2.34 Å, respectively. The optimized structure shows that **4** has tetrahedral geometry.

The frontier molecular orbitals of L and **4** are shown in Figures 5 and 6, respectively. In L, HOMO is spread over part of ligand moiety and LUMO spread over the whole ligand unit. After complexation with Zn(II), HOMO is spread over part of ligand unit whereas HOMO-1 is spread over chlorine atoms. The LUMO of **4** is spread over whole ligand unit. The HOMO-LUMO energy gaps of L and **4** was 4.33 and 3.27 eV. From the calculated values it can be concluded that **4** is more reactive than L. The results reveal that complexation results in the disruption of the internal charge transfer and resulted in the changes of electronic properties.

3.11. Molecular electrostatic potential (MEP)

The nucleophilic and electrophilic regions of the molecule can be identified using the molecular electrostatic potential map (MEP) [44, 45]. The structural properties of the molecules such as chemical reactivity of the compound can be described using these regions. The MEP of L and **4** are shown in Figure 7. A red color indicates electron rich sites, while the blue color represents electron deficient regions [46]. The azomethine nitrogen of the creatinine moiety is more electron rich region in the ligand. The central metal atom in **4** is more electron-rich site than the nitrogen atoms of the creatinine moiety. The electropositive sites are methyl group and methylene groups in ligand and **4**.

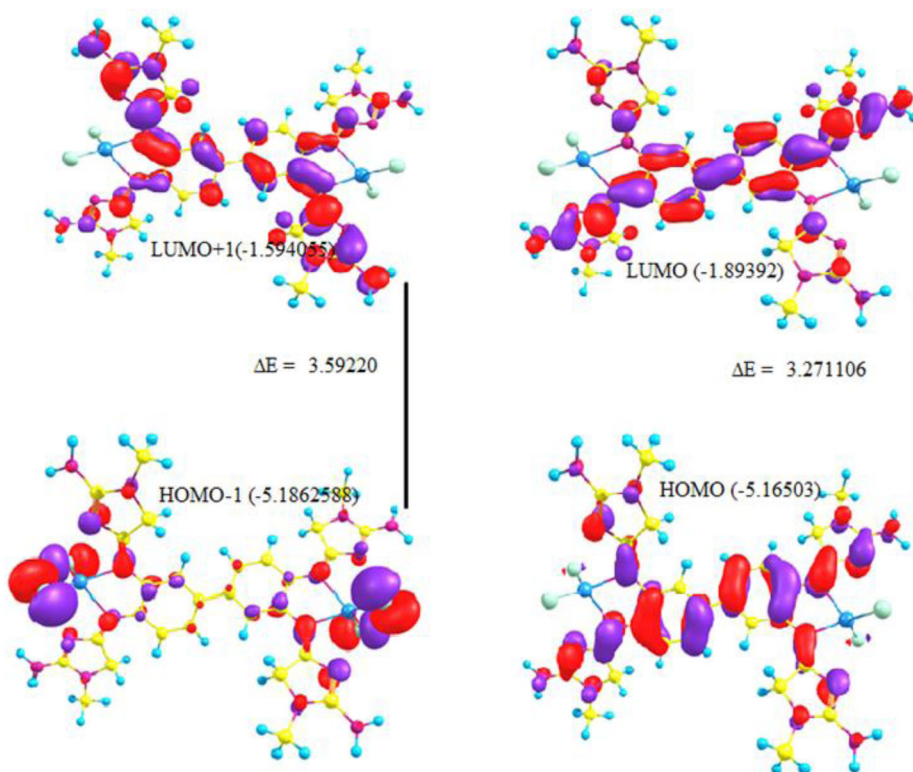


Figure 6. Frontier molecular orbital energies of Zn(II) complex.

3.12. Nonlinear optical (NLO) activity

NLO active materials are attracting great interest because of their potential applications in optoelectronic devices [47, 48] and THz wave generation [49]. THz region lying between microwave and infrared region offers wide applications which include inspection of drugs, wireless communications, spectroscopy, and imaging [50]. This wide range of applications of the materials increases interest in designing organic materials with desired nonlinear optical properties. The calculated polarizabilities and hyperpolarizabilities were taken from Gaussian output. The total static dipole moment (μ), static polarizability (α) and static hyperpolarizability (β_{tot}) have been stated [51] in [Supplementary Material](#) Equation (S1). The calculated first order hyperpolarizability (β_{tot}), mean polarizability ($\langle\alpha\rangle$) and dipole moment (μ) are given in [Table 2](#). Urea is one of the prototypical molecules used in the study of the NLO properties of molecular systems, and therefore, it was used as threshold value for comparative purpose. The first-order hyperpolarizability of L and **4** are 5.03 and 6.68 times larger than that of urea (1.3729×10^{-31} esu). The Schiff base complexes have improved NLO responses due to the metal atom which is placed at the center of charge-transfer system, compared to those of the free ligand.

3.13. Quantum chemical parameters

The Quantum chemical parameters such as (E_{HOMO}), (E_{LUMO}), ΔE , ionisation potential (I), electron affinity (A), chemical potential (μ), global hardness (η), global softness (S),

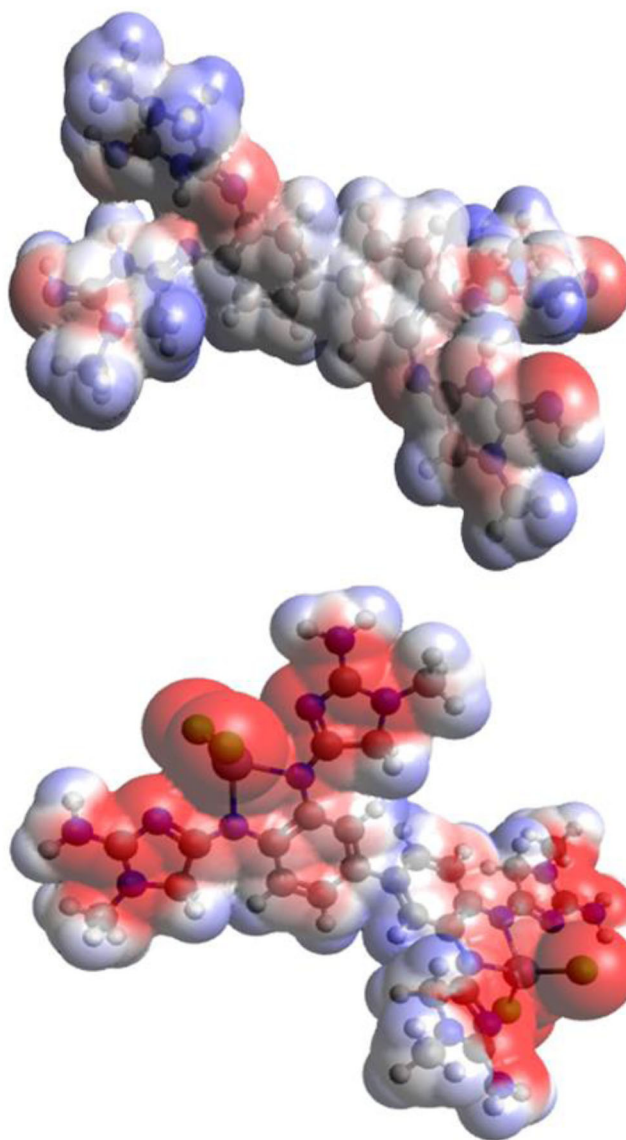


Figure 7. Molecular electrostatic potential (MEP) of Schiff base ligand and its Zn(II) complex.

Table 2. The polarizability (α), the first-order hyperpolarizability (β_{tot}) and their components for ligand L and Zn(II) complex **4**.

Compound	$\langle\alpha\rangle$ (a.u.)	$\Delta\alpha$ (a.u.)	β_{tot} (a.u.)	β_{tot} (esu)	$\beta_{\text{tot}}/\beta_{\text{tot}}$ (urea)
Ligand (L)	-243.8767	99.9481	80.0304	$6.91\text{E} - 31$	5.03
Complex 4	-172.4229	81.777	545.3229	$9.1795\text{E} - 31$	6.68
Urea	-21.5925	8.375	15.892	$1.3729\text{E} - 31$	1

electronegativity (χ), and global electrophilicity index (ω) were calculated for L and **4** and listed in [Supplementary Material Table S2](#).

The mentioned quantum chemical parameters were calculated with the help of the equations [52, 53] shown in [Supplementary Material Equation \(S2\)](#). The E_{total} of **4** was

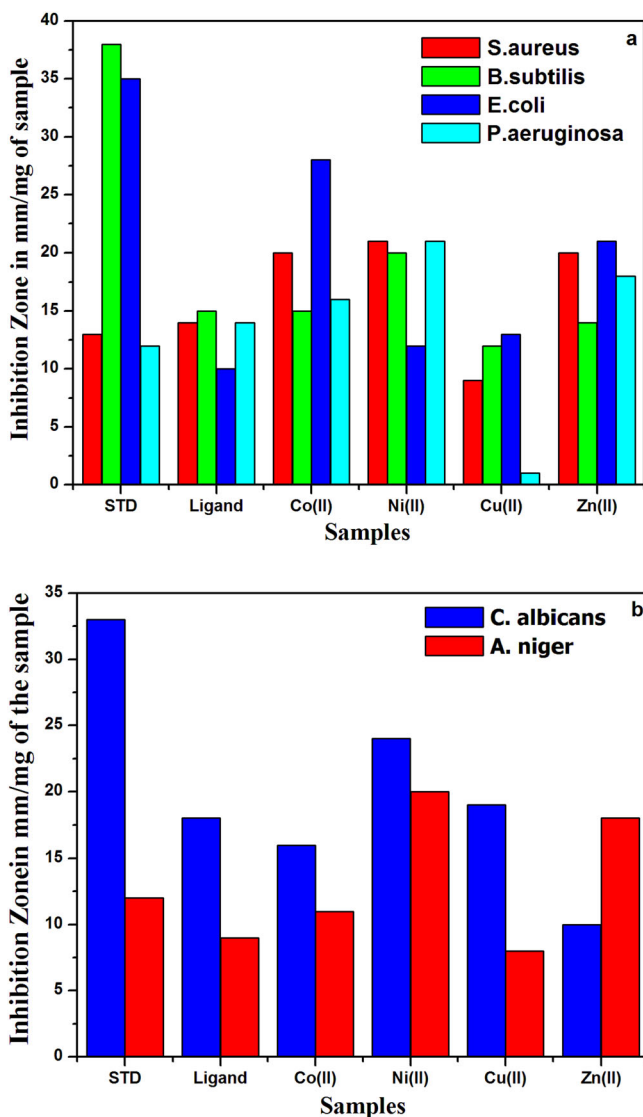


Figure 8. (a) Antimicrobial activity of Schiff base ligand and its metal complexes with different bacterial species. (b) Antimicrobial activity of Schiff base ligand and its metal complexes with different fungal species.

higher than the ligand, indicating the greater stability of the solid complex. The high electrophilicity index (ω) value indicates the good chance and priority for biological activity. The ligand molecule is capable of accepting electrons and its energy decreases upon accepting electronic charges was indicated by its positive electronegativity (χ) and negative electronic chemical potential values (μ) [54].

3.14. Antimicrobial activity

The Schiff base and its metal complexes were screened for their antimicrobial activity against *S. aureus* and *B. subtilis* as gram-positive bacteria, *E. coli* and *P. aeruginosa* as

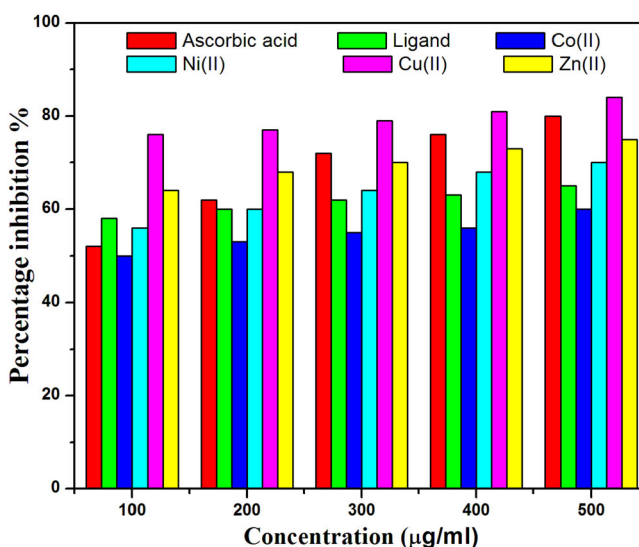


Figure 9. Concentration-dependent curves of antioxidant efficacy of Schiff base ligand and their metal complexes using L-ascorbic acid as standard and the methanolic DPPH solution as control.

gram-negative bacteria and *C. albicans* and *A. niger* as the fungus by disc agar diffusion method. The experimental data were compared with standards as shown in [Figure 8](#). The results show that the complexes have higher activity than the ligand against the similar microorganisms under the same experimental conditions. These results show that metal complexes are more potent in inhibiting the growth of microorganism than the Schiff base ligand except **3**, which has lower activity than the ligand against all the microorganisms except *E. coli*. The Co(II) and Zn(II) complexes showed good activity against *S. aureus* and *E. coli*. Complex **2** exhibits good activity against *S. aureus*, *B. subtilis*, and *P. aeruginosa* whereas it exhibits lower activity against *E. coli*. By comparing the results of antifungal activity of the Schiff base ligand and its complexes with the standard, it is obvious that the ligand and **1** and **3** showed lower activity against *A. niger*, except **2** and **4** which had moderate activity. Complex **2** exhibits good activity against *C. albicans* whereas **1** and **3** exhibit moderate activity.

The MIC values of **2** and **4** against *S. aureus*, *P. aeruginosa* and *A. niger* are given in [Supplementary material Table S3](#) and the results reveal that **2** (MIC = 62.5 µg mL⁻¹) shows good activity against *A. niger* and moderate activity against *P. aeruginosa* (MIC = 125 µg mL⁻¹). Complex **4** (MIC = 125 µg mL⁻¹) shows a moderate activity against the tested microorganisms *S. aureus*, *P. aeruginosa*, and *A. niger*.

The synthesized metal complexes showed difference in activities against various microorganisms due to impermeability into the microorganism cells. The size of the inhibition zone depends upon the culture medium, incubation conditions, rate of diffusion, and concentration of antibacterial agent. The activities of all the tested complexes may be explained on the basis of chelation theory [55, 56] where chelation reduces the polarity of the metal atom mainly because of partial sharing of the positive charge of the metal ion with the donor groups of the ligands and possible p-electron delocalization within the whole chelate ring. The low activity of some complexes

may be ascribed due to low lipid solubility, consequently the metal ion may not be able to reach favorable site of action of the cell wall to interfere with the normal cell activity. Though chelation dominates in assessing the biological behavior of the complexes, but simultaneously other factors such as dipole moment, size, bond length, geometry of complexes, concentration, coordination sites, and hydrophobicity have considerable influence on the antimicrobial potency. Hence it may be concluded that the antimicrobial activity of the complexes may not be due to chelation alone but it is convoluted blend of numerous contributions [57, 58].

3.15. Antioxidant activities

Free radicals play an important role in the inflammatory process. Many complexes have been reported as free radical inhibitors or radical scavengers in the literature. Schiff bases and its transition metal complexes exhibit significant antioxidant activity [59–61]. Hence we carried out systematic investigation to explore the antioxidant efficacy of free ligand and metal complexes by DPPH method using L-ascorbic acid (standard). The antioxidant data of the compounds at variable concentrations are shown in [Supplementary material](#) Table S4 and concentration-dependent curves are depicted in [Figure 9](#). The inhibitory effects of all the tested compounds are dose-dependent and the suppression ratio increases with increasing concentration. The DPPH-scavenging activity of **4** was higher than that of ascorbic acid. Complex **4** had significant scavenging effects with increasing concentration of 100–500 $\mu\text{g mL}^{-1}$. The scavenging activity of **4** is higher compared to ascorbic acid with IC_{50} values of 11.70 and 37.14 $\mu\text{g mL}^{-1}$ for **4** and ascorbic acid, respectively. The higher DPPH radical-scavenging activity is associated with the lower IC_{50} value. The IC_{50} values of ligand and **1–3** are 38.23, 91.30, 44.07, and 77.77 $\mu\text{g mL}^{-1}$, respectively, which is higher than that of ascorbic acid showing lower scavenging activity.

4. Conclusion

A binuclear Schiff base ligand (L) and its metal(II) complexes **1–4** have been synthesized and characterized using various spectroscopic techniques. All the complexes showed octahedral geometry except **4**, which had tetrahedral geometry. The presence of lattice water and coordinated water in metal complexes were analyzed using TGA/DTG analysis. The powder XRD shows sharp peaks, indicating microcrystalline structures. The SEM micrograms confirmed the homogeneous particle nature. The geometrical structure of Schiff base ligand and **4** were computed. From this, the bond angles, bond lengths, torsion angles and various other quantum chemical parameters were calculated. The synthesized ligand and their metal complexes were screened against Gram-(+) bacteria (*S. aureus* and *B. subtilis*), Gram-(–) bacteria (*E. coli* and *P. aeruginosa*) and fungal species (*C. albicans* and *A. niger*). Complexes **1**, **2**, and **4** had higher activities than the ligand against the bacterial species. The Ni(II) complex showed good activity against the fungal species compared with other metal complexes. The complexes showed enhanced activity than the parent ligand. The Zn(II) complex showed pronounced antioxidant activity compared to all other complexes.

Acknowledgements

This paper was supported by the KU Research Professor Program of Konkuk University.

Disclosure statement

No potential conflict of interest was reported by the authors.

ORCID

Mayakrishnan Prabakaran  <http://orcid.org/0000-0003-4759-0725>

References

- [1] C. Orvig, M.J. Abrams. *Chem. Rev.*, **99**, 2201 (1999).
- [2] N. Raman, S. Sobha, L. Mitu. *Monatsh. Chem.*, **143**, 1019 (2012).
- [3] S. Pandhaye, A. Zahra, S. Ekk. *Inorg. Chim. Acta*, **358**, 2023 (2005).
- [4] S. Kiran, S.B. Manjeet, T. Parikshit. *Eur. J. Med. Chem.*, **41**, 147 (2006).
- [5] S. Chakraborty, R.H. Laye, R.L. Paul, R. Gonnade, V.G. Puranik, M.D. Ward, G.K. Lahiri. *J. Chem. Soc. Dalton Trans.*, **6**, 1172 (2002).
- [6] A. Erxleben, J. Hermann. *J. Chem. Soc. Dalton Trans.*, **4**, 569 (2000).
- [7] W.H. Wang, G.X. Jin. *Inorg. Chem. Commun.*, **9**, 548 (2006).
- [8] M. Sheb. *Spectrochim. Acta, Part A*, **70**, 850 (2008).
- [9] M. Hobady, T.D. Smith. *Coord. Chem. Rev.*, **311**, 9 (1972).
- [10] I. Yoon, M. Narita, T. Shimizu, M. Asakawa. *J. Am. Chem. Soc.*, **126**, 16740 (2004).
- [11] H. Chen, D. Han, H. Yan, W. Tang, Y. Yang, H. Wang. *Polyhedron*, **12**, 1097 (1993).
- [12] M.L. Wang, F.Y. Wang, Z.Q. Li, X.Z. Li, D. Xu, D.Q. Qu. *Transit. Met. Chem.*, **26**, 307 (2001).
- [13] P. Tarasconi, S. Capacchi, G. Pelosi, M. Cornia, R. Albertini, A. Bonati, P.P. Dall'Aglio, P. Lughini, S. Pinelli. *Bioorg. Med. Chem.*, **8**, 157 (2000).
- [14] H. Singh, L.D.S. Yadav, S.B.S. Mishra. *J. Inorg. Nucl. Chem.*, **43**, 1701 (1981).
- [15] J. Charo, J.A. Lindencrona, L.M. Carlson, J. Hinkula, R. Kiessling. *J. Virol.*, **78**, 11321 (2004).
- [16] M. Kanthimathi, A. Dhathathreyan, B.U. Nair. *Chem. Phys. Lett.*, **324**, 43 (2000).
- [17] H. Zhang, Y. Zhang, C. Li. *J. Catal.*, **238**, 369 (2006).
- [18] B. Bahramian, V. Mirkhani, M. Moghadam, S. Tangestaninejad. *J. Appl. Catal. A*, **301**, 169 (2006).
- [19] S. Tabassum, M. Zaki, F. Arjmand, I. Ahmad. *J. Photochem. Photobiol. B*, **114**, 108 (2012).
- [20] V. Lozan, C. Loose, J. Kortus, B. Kersting. *Coord. Chem. Rev.*, **253**, 2244 (2009).
- [21] S.A. Sallam. *Transit. Met. Chem.*, **31**, 46 (2006).
- [22] G.M.J. Frisch, G.W. Trucks, H.B. Schlegel, G.E. Scuseria, M.A. Robb, J.R. Cheeseman, A. Scalmani, V. Barone, B. Mennucci, G.A. Petersson, H. Nakatsuji, M. Caricato, X. Li, H.P. Hratchian, J.F. Izmaylov, J. Bloino, G. Zheng, J.L. Sonnenberg, M. Hada, M. Ehara, K. Toyota, R. Fukuda, J.E. Hasegawa, M. Ishida, T. Nakajima, Y. Honda, O. Kitao, H. Nakai, T. Vreven, J.A. Montgomery, Jr., J. Peralta, F. Ogliaro, M. Bearpark, J.J. Heyd, E. Brothers, K.N. Kudin, V.N. Staroverov, R. Kobayashi, J.M. Normand, K. Raghavachari, A. Rendell, J.C. Burant, S.S. Iyengar, J. Tomasi, M. Cossi, N. Rega, R.E. Millam, M. Klene, J.E. Knox, J.B. Cross, V. Bakken, C. Adamo, J. Jaramillo, R. Gomperts, K.M. Stratmann, O. Yazyev, A.J. Austin, R. Cammi, C. Pomelli, J.W. Ochterski, R.L. Martin, J.B.V.G. Zakrzewski, G.A. Voth, P. Salvador, J.J. Dannenberg, S. Dapprich, A.D. Daniels, O. Farkas, D.J.F. Foresman, J.V. Ortiz, J. Cioslowski. *Gaussian 09*. Gaussian, Inc., Wallingford, CT (2009).
- [23] J. Wiecek, V. Dokorou, Z. Ciunik, D. Kovala-Demertzi. *Polyhedron*, **28**, 3298 (2009).
- [24] S.Y. Ebrahimipour, I. Sheikhsaie, J. Simpson, H. Ebrahimnejad, M. Dusek, N. Kharazmi, V. Eigner. *New J. Chem.*, **40**, 2401 (2016).

- [25] A. Ansari, M.K. Haris, A.K. Aijaz, S. Asfia. *Biol. Med.*, **3**, 141 (2011).
- [26] N. Vukovic, S. Sukdolak, S. Solujic, N. Niciforovic. *Food Chem.*, **120**, 1011 (2010).
- [27] R. Ramesh, P.K. Suganthy, K. Natarajan. *Synth. React. Inorg. Met.-Org. Chem.*, **26**, 47 (1996).
- [28] M.M. Abo-Aly, A.M. Salem, M.A. Sayed, A.A. Abdel Aziz. *Spectrochim. Acta Part A*, **136**, 993 (2015).
- [29] M.M. Aboaly, M.M.H. Khalil. *Spectrosc. Lett.*, **34**, 495 (2001).
- [30] A.A. Abou-Hussein, W. Linert. *Spectrochim. Acta Part A*, **141**, 223 (2015).
- [31] G.Y. Nagesh, K. Mahendra Raj, B.H.M. Mruthyunjayaswamy. *J. Mol. Struct.*, **1079**, 423 (2015).
- [32] A.Z. El-Sonbati, M.A. Diab, A.A. El-Bindary, M.I. Abou-Dobara, H.A. Seyam. *J. Mol. Liq.*, **218**, 434 (2016).
- [33] W.H. Mahmoud, R.G. Deghadi, G.G. Mohamed. *Appl. Organometal. Chem.*, **30**, 221 (2016).
- [34] N. Raman, R. Jeyamurugan, R. Senthilkumar, B. Raj Kapoor, S.G. Franzblau. *Eur. J. Med. Chem.*, **45**, 5438 (2010).
- [35] S. Chandra, S. Bargujar, R. Nirwal, N. Yadav. *Spectrochim. Acta Part A*, **106**, 91 (2013).
- [36] G. Kumar, S. Devi, D. Kumar. *J. Mol. Struct.*, **1108**, 680 (2016).
- [37] P. Tyagi, S. Chandra, B.S. Saraswat. *Spectrochim. Acta Part A*, **134**, 200 (2015).
- [38] U. Kumar, S. Chandra. *J. Saudi Chem. Soc.*, **15**, 187 (2011).
- [39] S. Ilhan, H. Baykara, A. Oztomsuk, V. Okumus, A. Levent, M.S. Seyitoglu, S. Ozdemir. *Spectrochim. Acta Part A*, **118**, 632 (2014).
- [40] A.B.P. Lever. *Inorganic Electronic Spectroscopy*, 2nd edn, Elsevier Science, Amsterdam (1984).
- [41] M.S. Refat, M.Y. El-Sayed, A.A. Adam. *J. Mol. Struct.*, **1038**, 62 (2013).
- [42] E. Akila, M. Usharani, S. Ramachandran, P. Jayaseelan, G. Velraj, R. Rajavel. *Arab. J. Chem.*, **10**, 2950 (2017).
- [43] C.J. Dhanaraj, J. Johnson. *Spectrochim. Acta Part A*, **118**, 624 (2014).
- [44] F.J. Luque, J.M. López, M. Orozco. *Theor. Chem. Acc.*, **103**, 343 (2000).
- [45] T.U. Devi, S. Priya, S. Selvanayagam, K. Ravikumar, K. Anitha. *Spectrochim. Acta Part A*, **97**, 1063 (2012).
- [46] Z. Nisa, A. Gul, Z. Akhter, M.A. Nadeem, M.N. Tahir, M.U. Ahmed. *J. Organomet. Chem.*, **820**, 130 (2016).
- [47] P.N. Parasad, D.J. Williams. *Introduction to Nonlinear Optical Effects in Molecules and Polymers*. John Wiley & Sons, New York 1991.
- [48] F. Kajzar, K.S. Lee, A.K.Y. Jen. *Adv. Polym. Sci.*, **161**, 1 (2003).
- [49] V. Krishnakumar, R. Nagalakshmi. *Physica B*, **403**, 1863 (2008).
- [50] J.V. Ramaclaus, T. Thomas, S. Ramesh, P. Sagayaraj, E.A. Michael. *Cryst. Eng. Commun.*, **16**, 6889 (2014).
- [51] H. Alyar, Z. Kantarci, M. Bahat, E. Kasap. *J. Mol. Struct.*, **834–836**, 516 (2007).
- [52] A.Z. El-Sonbati, G.G. Mohamed, A.A. El-Bindary, W.M.I. Hassan, M.A. Diab, S.M. Morgan, A.K. Elkholy. *J. Mol. Liq.*, **212**, 487 (2015).
- [53] E. Üstün, M. Çol Ayvaz, M. Sönmez Çelebi, G. Aşçı, S. Demir, İ. Özdemir. *Inorg. Chim. Acta*, **450**, 182 (2016).
- [54] A.Y. Al-Dawood, N.M. El-Metwaly, H.A. El-Ghamry. *J. Mol. Liq.*, **220**, 311 (2016).
- [55] O.A.M. Ali. *Spectrochim. Acta Part A*, **121**, 188 (2014).
- [56] B.G. Tweedy. *Phytopathology*, **55**, 910 (1964).
- [57] L.P. Nitha, R. Aswathy, N.E. Mathews, B.S. Kumari, K. Mohanan. *Spectrochim. Acta Part A*, **118**, 154 (2014).
- [58] K. Mohanan, S.N. Devi, B. Murukan. *Synth. React. Inorg. Met.-Org. Nano-Met. Chem.*, **36**, 441 (2006).
- [59] R.N. Patel, N. Singh, V.L.N. Gundla. *Polyhedron*, **26**, 757 (2007).
- [60] J. Labuda, L. Feníková, Z. Ďuračková. *Bioelectrochem. Bioenergy*, **44**, 31 (1997).
- [61] U. Weser, L.M. Schubotz, E. Lengfelder. *J. Mol. Catal.*, **13**, 249 (1981).